Chemical Science

ROYAL SOCIETY OF CHEMISTRY

EDGE ARTICLE

View Article Online
View Journal | View Issue

Cite this: *Chem. Sci.*, 2020, **11**, 9617

All publication charges for this article have been paid for by the Royal Society of Chemistry

A supramolecular aggregation-based constitutional dynamic network for information processing†

Xiao Lin,[a] Shu Yang,[b] Dan Huang,[a] Chen Guo,[a] Die Chen,[b] Qianfan Yang *[a] and Feng Li *[a]

Received 18th June 2020
Accepted 20th August 2020

DOI: 10.1039/d0sc03392h

rsc.li/chemical-science

Concepts and strategies offered by constitutional dynamic chemistry (CDC) hold great promise for designing molecular computing systems adaptive to external environments. Despite demonstrable success in storing and processing chemical information using CDC, further employment of such constitutional dynamic networks (CDNs) for processing more complex digital information has not been realized yet. Herein, we introduced a supramolecular CDN based on the aggregation of cyanine **MTC** (Agg-CDN), which is composed of four reversibly interconvertible constituents, *i.e.* monomers, dimers, J-aggregates, and H-aggregates. We demonstrated that the equilibrated Agg-CDN is reconfigurable through constituent exchange in response to well-defined chemical inputs. More importantly, the equilibrated states of the Agg-CDN are spectroscopically distinguishable because of the unique optical properties of **MTC**. We further tuned the Agg-CDN to at least nine unique states for transforming the chemical inputs into digital outputs, and successfully employed it for encoding and encrypting complex digital information, such as multi-pixel images.

Introduction

Molecular computing may serve as a promising alternative for information processing.[1–4] Compared to silicon-based computer technologies, molecular computing may facilitate in developing smaller and more efficient information devices.[5–7] Moreover, molecular computers are composed of reaction networks made of diverse chemicals or biomolecules. Therefore, they may respond directly to physical,[8] chemical,[9–11] or biological stimuli,[12] and lead to the development of intelligent computing systems which are adaptive to external stimuli.[13,14]

The adaptive nature of molecular computing systems echoes the emerging field of constitutional dynamic chemistry (CDC).[15,16] CDC can be realized using either reconfigurable chemical bonding,[17,18] a subfield known as dynamic covalent chemistry (DCC), or component-exchange among supramolecular entities.[19,20] In recent years, numerous constitutional dynamic networks (CDNs) operated using either DCC or supramolecular systems have been designed and adapted for processing chemical information.[21–23] For example, Lehn *et al.* constructed a CDN based on a dynamic covalent library of imines and acylhydrazones, which can store, recall and erase chemical information, *i.e.* the presence/absence of Zn^{2+} and Cu^{2+}.[24] In order to improve the information capacity, a CDN based on acylhydrazones was further constructed, with the ability to memorize diversified information including Zn^{2+}, Et_3N and light irradiation.[25] Moreover, to expand the realizable functions, a heterogeneous imine-based CDN was designed to implement pattern generation and information transformation in response to ten metal cations.[26]

Despite the success in using CDNs for storing and processing chemical information, further transformation to binary digital information for subsequent logic functions witnesses very limited efforts. Thus motivated by this, we introduced a supramolecular CDN based on cyanine aggregation (Agg-CDN), which is composed of four reversibly interconvertible constituents, *i.e.* monomers, dimers, J-aggregates, and H-aggregates (Fig. 1A). We demonstrated that the equilibrated Agg-CDN is reconfigurable through constituent exchange in response to well-defined chemical inputs. More importantly, the equilibrated states of the Agg-CDN are spectroscopically distinguishable because of the unique optical properties of cyanines thus allowing at least nine distinguishable Agg-CDN states for transforming the chemical inputs into digital outputs. By doing so, we successfully employed the Agg-CDN for encoding and encrypting complex digital information, such as multi-pixel images.

[a]*College of Chemistry, Sichuan University, Chengdu, 610064, China. E-mail: yangqf@scu.edu.cn; fli@brocku.ca*

[b]*West China School of Pharmacy, Sichuan University, Chengdu, 610041, China*

† Electronic supplementary information (ESI) available: All the DNA sequences used in this study; synthesis and characterization of **MTC**; detailed spectrogram in the experiment. See DOI: 10.1039/d0sc03392h

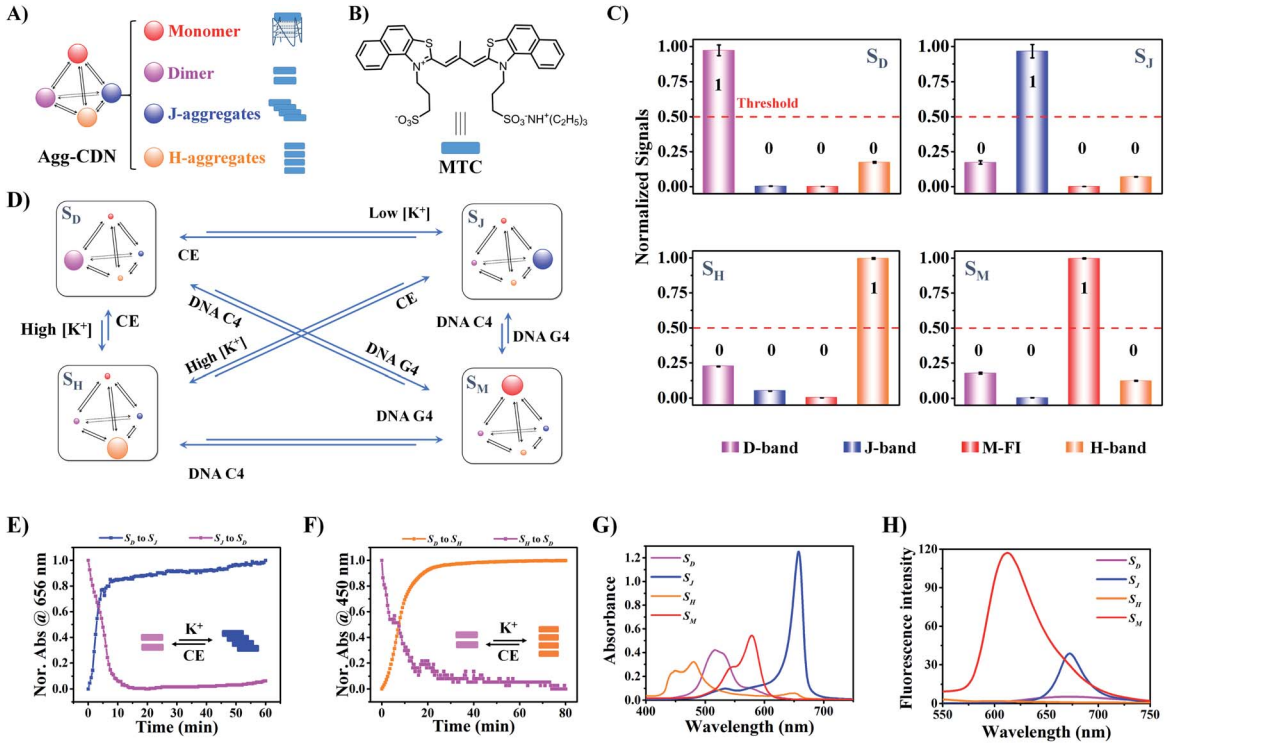

Fig. 1 Scheme of the Agg-CDN construction. (A) The Agg-CDN consisting of four interconvertible constituents (spheres), *i.e.* monomer (red), dimer (pink), J- (blue) and H-aggregates (orange). (B) The molecular structure of **MTC**. (C) The normalized spectral signal patterns of the four states of the Agg-CDN: (a) S_D, (b) S_J, (c) S_H and (d) S_M. The red dashed lines are the predefined threshold. (D) The dynamic conversion among the four specific distribution states of the Agg-CDN responding to external perturbations. (E) The kinetic curves of the reversible conversion between S_D and S_J with KCl or CE. (F) The kinetic curves of the reversible conversion between S_D and S_H with KCl or CE. (G) The absorption spectra of the four states of the Agg-CDN. (H) The fluorescence spectra of the four states of the Agg-CDN.

Results and discussion

Design of the Agg-CDN

The Agg-CDN was designed using a cyanine **MTC** [3,3′-di(3-sulfopropyl)-4,5,4′,5′-dibenzo-9-methyl-thiacarbocyanine triethylammonium salt] (the molecular formula is shown in Fig. 1B) as the building block. **MTC** has the tendency to self-assemble into various supramolecular aggregates in aqueous solutions, the concentration distribution of which is responsive to external chemical inputs.[27–30] Specifically, metal cations with various species and concentrations can dramatically regulate the aggregation distribution of **MTC** because of the metal-specific interactions and the solvent's dielectric constant perturbation due to ionic strength.[31–33] As is shown in Fig. S9,† in pH 8.5 Tris–Ac buffer solution with a very low K^+ concentration (less than 2 mM), **MTC** exists mainly as dimers, exhibiting a primary absorption peak at 515 nm (termed D-band). This state of the Agg-CDN is defined as S_D. At higher K^+ concentration (like 10 mM), the Agg-CDN is dominated by J-aggregates (defined as S_J), showing a sharp and strong absorption peak around 656 nm (termed J-band). Upon further increasing the concentration of K^+, the dominant constituent can shift to H-aggregates, evidenced by the gradual decrease of the **MTC** J-band and an increase in absorbance in the range of 420 nm to 480 nm (termed H-band). The CDN dominated by H-aggregates is defined as S_H. In addition to K^+, the Agg-CDN is also responsive to DNA G-quadruplexes (G4s). We have previously found that parallel/hybrid G4s could disassemble **MTC** dimers and J- and H-aggregates to monomers, where a characteristic fluorescence enhancement at 612 nm (termed M-Fl) could be observed (Fig. S10–S12†).[34] The Agg-CDN dominated by monomers was then defined as S_M.

Despite the fact that both J- and H- aggregates contain mixtures of aggregates with various sizes,[31] we found that S_J and S_H remain spectroscopically distinguishable (Fig. 1C). Therefore, we were able to quantify the concentrations of each constituent in any state through external calibration (Fig. S8 and Table S3†).

More importantly, all the states of the Agg-CDN are reversible (Fig. 1D). For example, the transition from S_D to S_J was completed within 10 min by increasing the K^+ concentration, whereas the reverse transition was rapidly achieved by chelating K^+ using 18-crown-6 (CE) (Fig. 1E and S13†). A rapid kinetic profile was also observed for the interconversion between S_D and S_H (Fig. 1F). Similarly, G4s could promote the transformation of S_J to S_M while complementary cytosine-rich DNAs (C4s) can suppress the formation of G-quadruplexes and thus reverse this process (Fig. S14 and S15†). To ensure that all the reactions in the Agg-CDN reach equilibrium upon measurement, a 90 min incubation was set for all the subsequent reactions throughout the study.

As shown in Fig. 1G and H, all four Agg-CDN states, S_M, S_D, S_J and S_H, are spectroscopically distinguishable, because of the exciton delocalization effect of **MTC** supramolecular

aggregation. In addition, the transition between any two Agg-CDN states may also be monitored by resolving a mixed spectrum. By doing so, we have achieved as many as nine spectroscopically distinguishable CDN states which store specific combinations of two external chemical inputs, including K^+ and a G4 oligonucleotide named Code (Fig. 2). The further transformation of the chemical information stored in the Agg-CDN to binary signals was achieved *via* setting a threshold (red dashed lines in Fig. 1C) for the normalized **MTC** spectral signals. We defined the normalized signals greater than the threshold as "1", otherwise as "0". By assigning the binarized J-band, M-FI and H-band as the 1st, 2nd and 3rd bit values, respectively, we were able to finally transform the chemical information into three-bit digital information though the Agg-CDN (Fig. 2).

Molecular computing of the Agg-CDN

The power of the Agg-CDN for molecular computing was next demonstrated by performing image encoding and decoding operations, the two-way conversions between black-and-white pixels and chemical information (Fig. 3A). In a typical workflow (Fig. 3B), a graphic of letter "S" was first divided into units of three-pixel patterns. As defined in Fig. 2, each pattern corresponds to one specific state of the Agg-CDN, which also stores a specific combination of K^+ and Code inputs. Through the Agg-CDN, chemical information can be converted to a specific image and *vice versa*. A similar principle can be scaled up to encode/decode patterns with a much larger footprint and complexity. For example, we demonstrated that the panda logo for the World Wide Fund for Nature (WWF) with 108 units could also be encoded by arranging varying states of the Agg-CDN in the same manner (Fig. 3C and S16–S21†).

Having established the functions of encoding and decoding, we further applied the Agg-CDN to more complicated image processing operations, encryption and decryption (Fig. 4A and S22†). As shown in Fig. 4B and S23,† the encryption is achieved by reconfiguring all abovementioned eight CDN states (termed

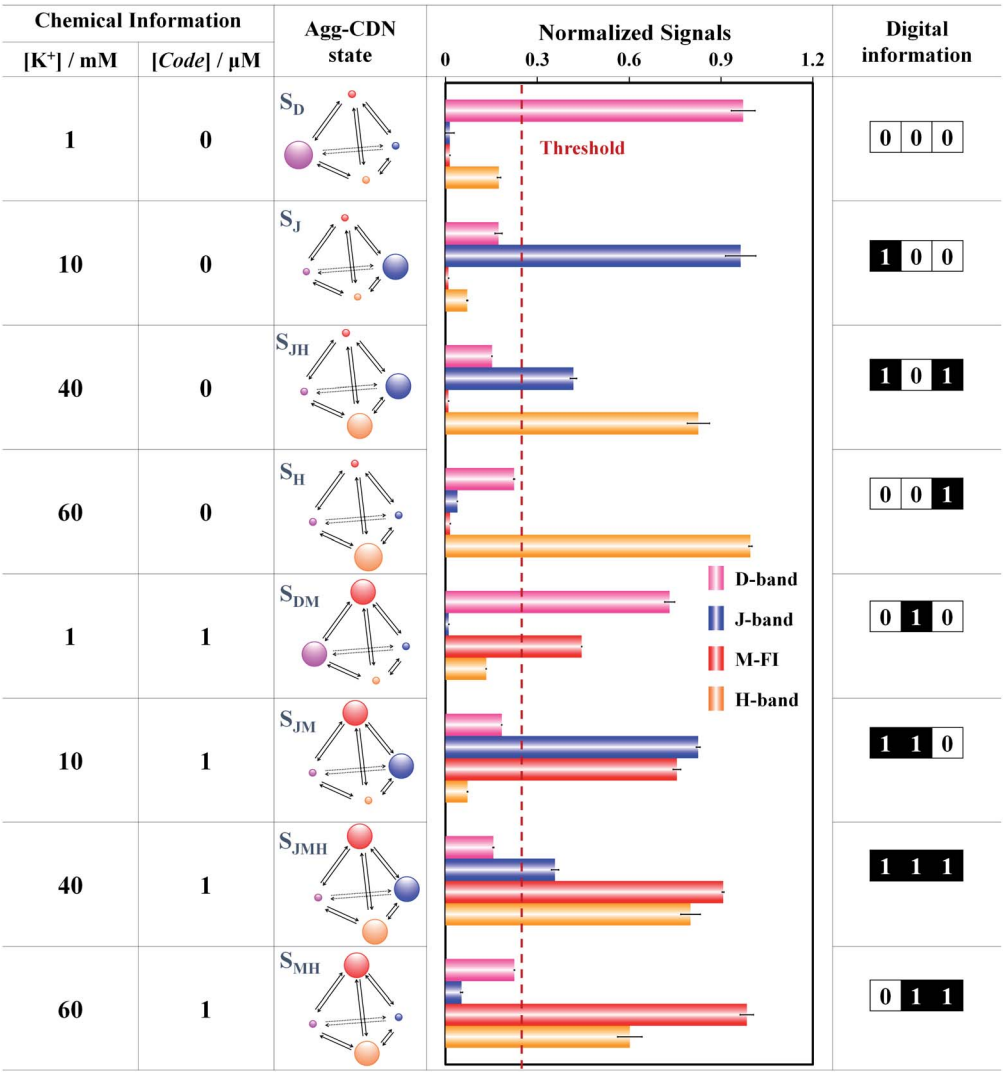

Fig. 2 The transformation of chemical information into three-bit digital information *via* the Agg-CDN. The combination of two external chemical inputs, K^+ and Code, can tune the Agg-CDN to various spectroscopically distinguishable states, including S_D, S_J, S_{JH}, S_H, S_{DM}, S_{JM}, S_{JMH} and S_{MH}. And each state can be directly read out as the digital values using the normalized signal pattern.

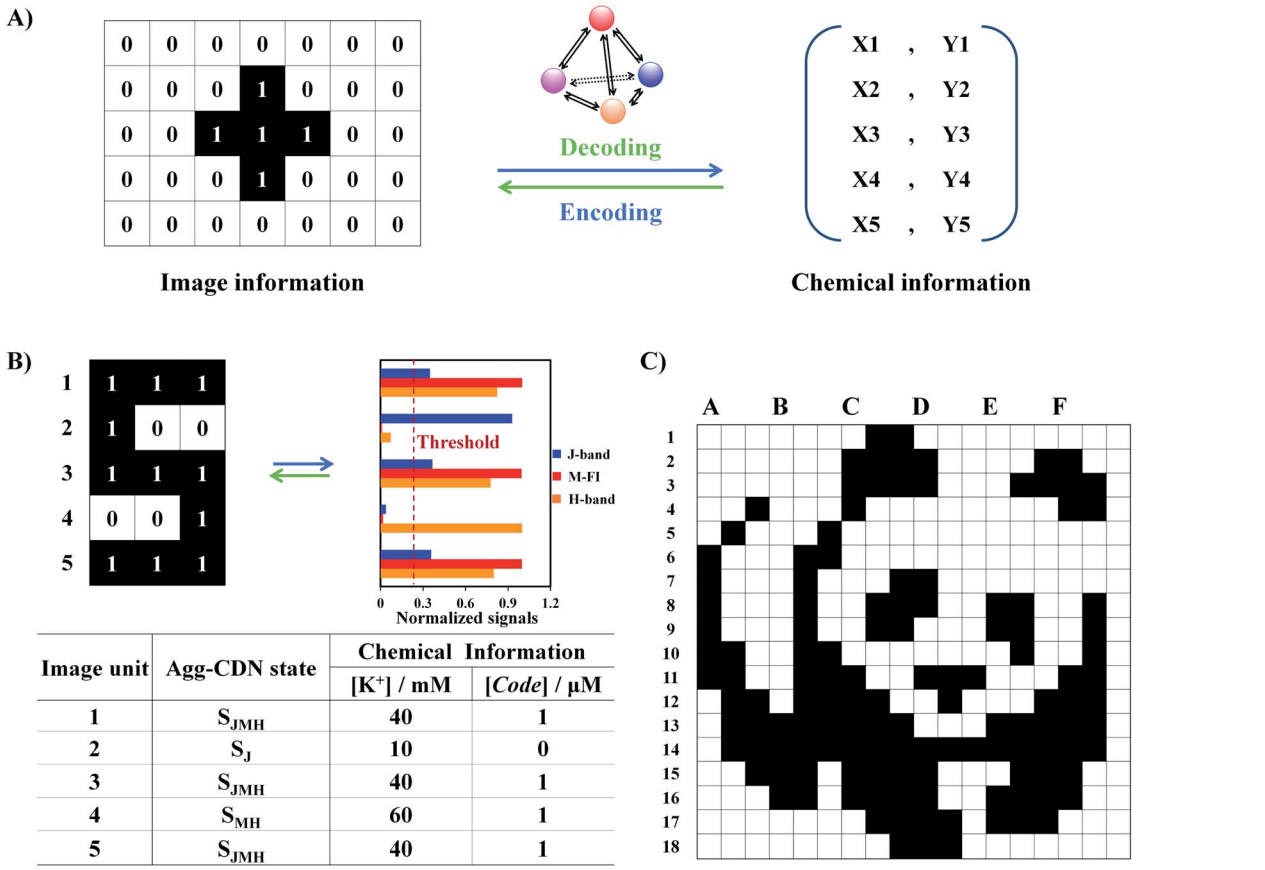

Image unit	Agg-CDN state	Chemical Information	
		[K⁺] / mM	[*Code*] / μM
1	S_{JMH}	40	1
2	S_J	10	0
3	S_{JMH}	40	1
4	S_{MH}	60	1
5	S_{JMH}	40	1

Fig. 3 The operation of image encoding/decoding based on the Agg-CDN. (A) The schematic diagram of the image encoding and decoding processes *via* the Agg-CDN. Two examples of encoding/decoding black-and-white images using the Agg-CDN, including (B) the graphic of letter "S" and (C) the panda logo for the WWF.

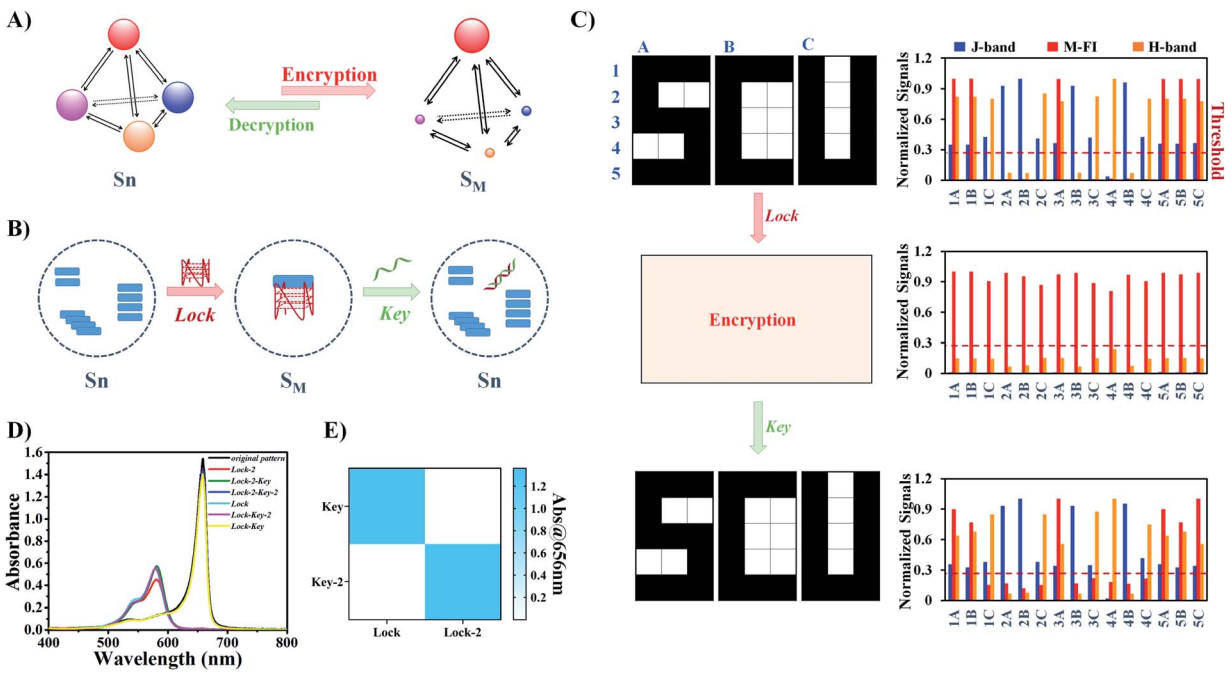

Fig. 4 The operations of the image encryption/decryption based on the Agg-CDN. (A) Encrypting the Agg-CDN function by tuning its state from Sn (n = D, J, JH, H, DM, JM, JMH and MH) to S_M. (B) The schematic diagram of the changes in the constituents (assemblies) of the Agg-CDN in image encrypting/decrypting processes. (C) An example of encrypting/decrypting a black-and-white graphic of the initialism of Sichuan University *via* the Agg-CDN. The absorbance spectra (D) and the heat map (E) of the two orthogonal encrypting/decrypting operations of the Agg-CDN.

Sn) into a unified S_M state by adding a 12 μM concentration of G4 strand Lock as a molecular lock. Spectroscopically, all the CDN states for image encoding are masked by the Lock strand, evidenced by a unified signal readout. Moreover, this encryption process is reversible. Upon the addition of a Key strand that is complementary to Lock, all the CDN states were restored without any loss of the original chemical information, allowing the accurate identification of the original image (Fig. 4C and S24†).

Having successfully demonstrated the encryption and decryption of one image using the pair of Lock/Key, we further demonstrated that other G4/C4 DNA pairs can be used to perform the same encrypting/decrypting operations to the same system (Fig. 4D, E and S25†). The multiple orthogonality of lock and key pairs provides a higher level of security in practice.

Conclusions

In conclusion, we have introduced a novel constitutional dynamic network (Agg-CDN) based on supramolecular aggregates. At least nine spectroscopically distinguishable states of the Agg-CDN can be finely tuned, which allows the high-density storage of specific chemical information, including varying combinations of K^+ and DNA G4 strands. Because of the unique design and spectroscopic properties, the Agg-CDN enables further encoding/decoding and encrypting/decrypting operations on complex digital information, such as multi-pixel images. Our study has demonstrated the possibility and potential for devising novel molecular computing systems using the principle of CDC. The success of designing the Agg-CDN by manipulating supramolecular aggregates may also inspire the design of new CDC systems.

Experimental section

Chemicals and materials

DNA oligonucleotides (listed in Table S1†) were purchased from Sangon Biotechnology Co. Ltd. (Shanghai, China). The cyanine dye **MTC** was synthesized in our lab according to the methods of the methods of Hamer[35] and Ficken,[36] and the purity was proved by high resolution mass spectrometry (HRMS), high performance liquid chromatography (HPLC), nuclear magnetic resonance (^{1}H NMR and ^{13}C NMR) and absorption spectroscopy. All the analytical reagent grade chemicals were purchased from Aldrich Ltd. (Shanghai, China) and used as received without further purification. Ultrapure water prepared using an ULUPURE (Chengdu, China) ultrapure water system and was used throughout the experiments.

Instruments and equipment

The absorption spectra were acquired using a 10 mm quartz cuvette on an EVOLUTION 201 spectrophotometer (Thermo Scientific, USA) at room temperature in a 10 mm quartz cell, and the scan range was 400–750 nm. The fluorescence spectra were collected with an F-4600 spectrophotometer (HITACHI, Japan) in a 10 mm quartz cell at room temperature, and a xenon arc lamp was used as the excitation light source. Both the excitation and emission slits were 5 nm, and the PMT voltage was 400 V. The excitation wavelength was 530 nm and emission wavelength was 530–750 nm.

Sample preparation

The Code stock solution was dissolved in 10 mM, pH 6.5 Tris–Ac buffer solution and the other DNA stock solutions were dissolved in 10 mM, pH 8.5 Tris–Ac buffer solution. The concentrations of DNA were determined by measuring absorbance at 260 nm. A 150 μM **MTC** stock solution was prepared by dissolving 7.67 mg **MTC** powder in 50 mL methanol and stored in the dark. The concentration of the **MTC** stock solution was corrected by diluting a 50 μL stock solution to 1000 μL with methanol, measuring its absorbance at 573 nm and calculating the actual concentration *via* Lambert-beer's law. The stock solution of KCl was diluted to 1 M using ultrapure water.

Experimental operations

The encoding and decoding operations. To demonstrate the image information processing of the Agg-CDN, the experimental conditions were optimized and metal ions and DNA strands were incubated with **MTC** in the dark at 37 °C before the measurement. To regulate the eight states of the Agg-CDN, 20 μL **MTC** stock solution (150 μM), metal ions, and Code were added into 10 mM, pH 8.5 Tris–Ac buffer solution. The total volume of the reaction sample was 500 μL. The final concentration of the ions was 1 μM Code with 1 mM K^+, 10 mM K^+, 40 mM K^+ and 60 mM K^+ or only four concentrations of K^+. When all the stock solution was added in, the samples were allowed to stand at room temperature for 5 min, fully mixed and then incubated at 37 °C in the dark for 90 min. The eight pairs of Code and K^+ were combined randomly corresponding to the encoded image.

The encryption and decryption operations. For the encryption operation, Lock was added to the samples in which encryption operation has been implemented. The concentration of Lock in each sample was 12 μM. After incubation at 37 °C in the dark for 90 min, absorption and fluorescence spectra were collected. For the decryption operation, an annealing step was performed first. Lock and Key (Lock-2 and Key-2) were incubated in the 10 mM, pH 8.5 Tris–Ac buffer solution in a concentration ratio of 1 : 1.2 at 90 °C for 5 min. The Lock–Key (Lock-2 and Key-2) complex was added to the samples in which decryption operation has been implemented. After incubation at 37 °C in the dark for 90 min, absorption and fluorescence spectra were collected. The flow chart for the encryption/decryption operations is shown in Fig. S18.†

Conflicts of interest

There are no conflicts to declare.

Acknowledgements

The kind assistance of Prof. Peng Wu and Dr Yani Xie from the Analytical & Testing Center at Sichuan University is greatly appreciated.

Notes and references

1 L. M. Adleman, *Science*, 1994, **266**, 1021–1024.
2 H. Tian, *Angew. Chem., Int. Ed.*, 2010, **49**, 4710–4712.
3 M. Amelia, L. Zou and A. Credi, *Coord. Chem. Rev.*, 2010, **254**, 2267–2280.
4 K. M. Cherry and L. Qian, *Nature*, 2018, **559**, 370–376.
5 M. Lv, W. Zhou, D. Fan, Y. Guo, X. Zhu, J. Ren and E. Wang, *Adv. Mater.*, 2020, **32**, e1908480.
6 D. Fan, J. Wang, E. Wang and S. Dong, *Chem. Sci.*, 2019, **10**, 7290–7298.
7 R. Orbach, S. Lilienthal, M. Klein, R. D. Levine, F. Remacle and I. Willner, *Chem. Sci.*, 2015, **6**, 1288–1292.
8 S. M. Chirieleison, P. B. Allen, Z. B. Simpson, A. D. Ellington and X. Chen, *Nat. Chem.*, 2013, **5**, 1000–1005.
9 D. Huang, C. Yang, Y. Yao, J. Li, C. Guo, J. Chen, Y. Zhang, S. Yang, Q. Yang and Y. Tang, *Chem.–Eur. J.*, 2019, **25**, 6996–7003.
10 D. Huang, C. Guo, J. Miao, Y. Zhang, X. Lin, D. Chen, S. Yang, Q. Yang and Y. Tang, *Nanoscale*, 2019, **11**, 16241–16244.
11 J. Chen, S. Yang, C. Yang, J. Li, D. Huang, X. Lin, C. Guo, Q. Zhou, Q. Yang and Y. Tang, *Chem.–Eur. J.*, 2019, **25**, 5691–5697.
12 Y. Benenson, *Nat. Rev. Genet.*, 2012, **13**, 455–468.
13 P. Zhang, D. Gao, K. An, Q. Shen, C. Wang, Y. Zhang, X. Pan, X. Chen, Y. Lyv, C. Cui, T. Liang, X. Duan, J. Liu, T. Yang, X. Hu, J. J. Zhu, F. Xu and W. Tan, *Nat. Chem.*, 2020, **12**, 381–390.
14 C. Liu, Z. Huang, W. Jiang, X. Liu, J. Li, X. Han, H. Tu, L. Qiu and W. Tan, *Anal. Chem.*, 2020, **92**, 3620–3626.
15 P. T. Corbett, J. Leclaire, L. Vial, K. R. West, J.-L. Wietor, J. K. M. Sanders and S. Otto, *Chem. Rev.*, 2006, **106**, 3652–3711.
16 J. M. Lehn, *Chem. Soc. Rev.*, 2007, **36**, 151–160.
17 S. P. Black, J. K. Sanders and A. R. Stefankiewicz, *Chem. Soc. Rev.*, 2014, **43**, 1861–1872.
18 Y. Jin, C. Yu, R. J. Denman and W. Zhang, *Chem. Soc. Rev.*, 2013, **42**, 6634–6654.
19 S. Wang, L. Yue and I. Willner, *Nano Lett.*, 2020, **20**, 5451–5457.
20 L. Yue, S. Wang, V. Wulf and I. Willner, *Nat. Commun.*, 2019, **10**, 4774.
21 P. Zhang, L. Yue, M. Vazquez-Gonzalez, Z. Zhou, W. H. Chen, Y. S. Sohn, R. Nechushtai and I. Willner, *ACS Nano*, 2020, **14**, 1482–1491.
22 L. Yue, S. Wang and I. Willner, *Sci. Adv.*, 2019, **5**, eaav5564.
23 Z. Zhou, X. Liu, L. Yue and I. Willner, *ACS Nano*, 2018, **12**, 10725–10735.
24 J. Holub, G. Vantomme and J. M. Lehn, *J. Am. Chem. Soc.*, 2016, **138**, 11783–11791.
25 G. Men and J. M. Lehn, *Chem. Sci.*, 2019, **10**, 90–98.
26 A. Osypenko, S. Dhers and J. M. Lehn, *J. Am. Chem. Soc.*, 2019, **141**, 12724–12737.
27 C. Yang, S. Yang, L. Song, Y. Yao, X. Lin, K. Cai, Q. Yang and Y. Tang, *Chem. Commun.*, 2019, **55**, 8005–8008.
28 C. Yang, L. Song, J. Chen, D. Huang, J. Deng, Y. Du, D. Yang, S. Yang, Q. Yang and Y. Tang, *NPG Asia Mater.*, 2018, **10**, 497–508.
29 C. Yang, D. Zou, J. Chen, L. Zhang, J. Miao, D. Huang, Y. Du, S. Yang, Q. Yang and Y. Tang, *Chem.–Eur. J.*, 2018, **24**, 4019–4025.
30 D. Chen, S. Yang, Z. Wu and X. Xu, *Chem.–Eur. J.*, 2020, DOI: 10.1002/chem.202001240.
31 H. X. Sun, J. F. Xiang, Q. F. Yang, Q. A. Shang, Q. J. Zhou, Y. X. Zhang, G. Z. Xu and Y. L. Tang, *Appl. Phys. Lett.*, 2011, **98**, 031103.
32 L. Wang, J. Xiang, H. Sun, Q. Yang, L. Yu, Q. Li, A. Guan and Y. Tang, *Dyes Pigm.*, 2015, **122**, 382–388.
33 H. Sun, J. Xiang, W. Gai, Y. Liu, A. Guan, Q. Yang, Q. Li, Q. Shang, H. Su, Y. Tang and G. Xu, *Chem. Commun.*, 2013, **49**, 4510–4512.
34 Q. Yang, J. Xiang, S. Yang, Q. Li, Q. Zhou, A. Guan, L. Li, Y. Zhang, X. Zhang, H. Zhang, Y. Tang and G. Xu, *Anal. Chem.*, 2010, **82**, 9135–9137.
35 F. M. Hamer, *The cyanine dyes and related compounds*, Interscience Publishers, New York, 1964.
36 G. E. Ficken, *The Chemistry of Synthetic Dyes*, Academic Press, New York, 1971.

